

MASS TRANSFER FROM DROPLETS
FALLING THROUGH A QUIESCENT BATH

BY
UDAY CHATTERJEE

511

ME

1971

M

CHA

MA



DEPARTMENT OF METEOROLOGICAL ENGINEERING
INDIAN INSTITUTE OF TECHNOLOGY KANPUR
JUNE 1971

CENTRAL LIBRARY
Indian Institute of Technology
KANPUR

Class No. **Thesis**
669.79
C 392

MASS TRANSFER FROM DROPLETS FALLING THROUGH A QUIESCENT BATH

A Thesis Submitted
in Partial Fulfillment of the Requirements
for the Degree of
MASTER OF TECHNOLOGY

BY
MOHAY CHATTERJEE



511

IN 1971

DEPARTMENT OF MECHANICAL ENGINEERING
INDIAN INSTITUTE OF TECHNOLOGY KANPUR
JUNE 1971

ME - 1971 - M - CHA - MAS



Continued

This is to certify that the study of "Streamline flow droplets falling through a quiescent liquid" has been carried out by Mrs. Uma Chakravarty under my supervision and that this work has not been submitted elsewhere for a degree.

A. Chakraborty

(in B.Sc.)

24/11/77, 120/11/77

Dr. A. Chakraborty

Indian Institute of Technology Kanpur



ABSTRACT

Transfer of Indium from falling mercury-indium amalgam droplets to a static bath of aqueous ferric chloride solution was investigated at 30°C. The viscosity of the aqueous solution was varied by addition of glycerol up to 75 wt percent. The reaction was



The droplet sizes were employed. The change of concentration of Fe^{3+} in the aqueous phase as a function of time was followed by sampling and polarographic analysis. The diffusion coefficient of ferric ion at various concentrations were measured by polarographic technique. The terminal velocity and residence time of the droplets were measured by photographic technique. Efforts were also made to get an idea of the droplet oscillation during their fall through aqueous phase. Kinetic considerations and mass-transfer calculations confirm aqueous control. However, $\log \frac{[Fe^{3+}]_0}{[Fe^{3+}]_t}$ shows some unexpected deviation from linearity when plotted against time. Variation of diffusion coefficient with concentration of ferric ion does not explain this departure from linearity completely. The drag coefficient vs Reynolds number behaviour is very close to that obtained by Calderbank et al and shows departure from solid sphere behaviour at high Reynolds number. The mass-transfer coefficient is one order magnitude higher than that expected from the solid sphere behaviour presumably due to droplet oscillation and possibly Marangoni effect. The droplets attained terminal velocity at a very short distance after the fall.

ACKNOWLEDGMENT

It has been a great pleasure to work on the project problem concerning the most important but hitherto overlooked aspect of desiccation in plant tissues. I am thankful to Dr. A. Baskin and Dr. J.B. Skene for advising this important and sensitive problem of today, and their generous and detailed assistance to meet the challenges encountered in successful completion of the work.

I am grateful to Dr. J.B. Skene for providing high quality facilities for micrographical study.

I am thankful to Dr. J.B. Skene for extending all facilities for using the Polarograph, and to Mr. Ferguson who trained me in handling the instrument.

I gratefully acknowledge Dr. F.B. Skene's help in selecting the separating liquid used in the work.

Dr. J.B. Skene's guidance in measuring terminal volume of droplets by electrical techniques is gratefully acknowledged.

Dr. J.B. Skene and Mr. J. Skene both Graduate Students deserve my sincere thanks for their help in doing the photographic work. I am grateful to Mr. A. Baskin and J.B. Skene, also graduate students for their help in cooperation work.

I am thankful to Mr. David Baskin and all the technicians of the Biophysics Workshop for their help in fabrication work. Class meeting sessions guarantee the whole credit for making the glass apparatus.

Services of Mr. J.B. Skene is acknowledged for the final stage of the work.

Table of Contents

Chapter	=	1	Introduction	...	2
Chapter	=	2	Fish and wildlife of the river	...	14
Chapter	=	3	Reservoirs and Irrigation Techniques	...	243
Chapter	=	4	Experimental	...	177
Chapter	=	5	Drainage	...	277
Chapter	=	6	Estuaries	...	311
Chapter	=	7	Coastal waters	...	404
References				...	423

1. INTRODUCTION

Since the development of the film mass transfer theory¹, Chemical Engineers have undertaken many fundamental studies on mass transfer from a drop phase to a surrounding liquid phase under different hydrodynamic conditions, various models have been developed which may be extended to specific metallurgical systems also.

In any blast furnace operation, iron-ore is reduced to iron and while coming down through the stack it picks up Si, Mn, S, P etc. from the burden. The molten iron in the form of droplets of different sizes passes through the hearth region and collects in the hearth. The slag that forms from the gangue materials collects at the top of the metal. In normal operation the quantity of slag is about 40-70% of the total iron tapped. So, it is expected that the metal is always covered with a thick layer of slag and all the droplets of iron has to cross the thick viscous layer before they are collected in the hearth.

The existence and formation of the droplets inside the blast furnace has been conclusively proved by many authors in the past. Schuster² while explaining the "Mechanism of the formation of iron shots in B.F and low shaft furnace slag" had given a good review of the previous work done in this field. Kosobrovitch³ explained

The Mechanism of desolvagization under R_1R_2 conditions on the basis of analysis and film theory and proved that mass transfer from droplets occurs in the slug phase.

1.1 The mass transfer between a single drop and the surrounding fluid will depend on the

- (i) Shape and the nature of the drop
- (ii) Motion of the drop in the medium
- (iii) Diffusional flux on the surface.

1.1a Shape and nature of the drop

There are many situations when the liquid droplets passing through the continuous phase can not maintain its original shape. The shape will be ellipsoidal and will oscillate along the major axis. Large drops can be considered to be oblate spheroid which may even oscillate to approximate prolate spheroidal shape¹. The oscillating drops show far greater rate of mass transfer than any other type. Quinn² observed that when the drop density is very high and the ratio of the drop viscosity to the aqueous phase viscosity is very small, then the drop may assume the prolate shape. The eccentricity ratio E^1 is expressed by the author as

$$E^1 = \frac{\partial x}{\partial t} \left(1 + \frac{\partial x}{\partial t} \right) = \frac{1}{2} \left\{ \frac{1}{3} + \frac{2}{5} \left(\frac{\partial x}{\partial t} \right) + \frac{1}{7} \left(\frac{\partial x}{\partial t} \right)^2 + \frac{1}{9} \left(\frac{\partial x}{\partial t} \right)^3 \right\} - \dots \quad (1)$$

When E^1 is greater than 0, the distortion is prolate

and if $E^1 < 0$, the distortion is oblate.³

* Visit the list of nomenclatures given at the end of the text for explanation of the terms.

As the drop size increases, the eccentricity of the nonoscillating ellipsoidal drop increases. Garner and Cowker² prepared the equation for calculating the area of such nonoscillating drop.

$$A = \frac{\pi}{2} \left[a^2 + \frac{b^2}{e^2-1} \ln \left(e + \sqrt{e^2-1} \right) \right] \quad (2)$$

The ratio of the area of an ellipsoid to that of a sphere of equal volume is

$$\frac{A}{A_0} = 1 + \left[\frac{b^2}{e^2-1} \ln \left(e + \sqrt{e^2-1} \right) \right] \quad (3)$$

If the drop of low viscosity moves through a high viscous field a series of shape change is expected. The shape of the droplet affects the Sherwood number in a complex way, but the mass-transfer co-efficient remains proportional to the (diffusivity)^{1/2} and agrees well with the theoretical analysis of transfer across mobile interfaces⁴.

When the size of a drop falling in a low viscosity medium is increased beyond the laminar flow region, the drop begins to oscillate. The term oscillation refers to periodic changes from oblate ellipsoid to prolate and back to original form along the axis of symmetry. Sanchez and Cowker² developed the equation by using the primary mode of oscillation and expressed as:

$$\omega = \Omega = \left[\frac{19.3 G^2 \gamma}{(\rho^2 \nu^2 R_0^3) a_0^2} \right]^{1/4} \quad (4)$$

1.1 b. Motion of the drop

The motion of the liquid drop in the liquid medium has been studied extensively by Chemical Engineers as a part of liquid-liquid extraction technique. The motion of liquid mercury droplets in electrolytic solution is characterized by the existence of charges on the liquid surface. The motion of liquid droplets in the liquid medium is closely tied up with the size of the diffusional film to the drop solution interface.

The effect of surface active material on the motion of drop had been studied by Levinsk and Goussakov.⁷ It was observed that surface active materials may retard the motion on the surface of the drop when drop size is small. The surface active materials cannot retard the surface motion of a relatively large drop. Therefore, even in a medium containing such material, a large sized drop falls under the condition of unretarded surface motion. A model had been proposed by Tsang and Kulkarni⁸ which accounted for the reduced mass transfer to drop falling in medium containing surface active agents. The reduction in the interfacial area and change in velocity and circulation pattern were the causes of reduced mass-transfer. The theoretical and experimental values agreed with each other well within 10%.

For a spherical liquid drop moving in another liquid field, the boundary does not remain rigid. It moves from front to rear stagnation along the axis of symmetry, creating continuously a new area. Hohenberg and Edmard had shown that a change in boundary condition on the surface of a drop leads to a significant change in the velocity of the falling drops. For the fall of a small liquid drop in a liquid medium under the gravitational force, ρ_1 , the terminal settling velocity had been expressed as

$$v = \frac{2}{9} \frac{r^2 (\rho_1 - \rho_2)}{\mu_2} \cdot \frac{\rho_2 + \rho_1}{2\rho_2 + \rho_1} C_{cor} / \text{cm} \quad (5)$$

When the viscosity of the exterior liquid is large, $\mu_2 \gg \mu_1$ the equation reduces to:

$$v = \frac{2}{9} \frac{r^2 (\rho_1 - \rho_2)}{\mu_2} \quad (6)$$

which is Stoke's law. The Stokes law correction factor for liquid drop had been calculated from analysis of Edmard and Hohenberg⁶ and expressed as:

$$C_{cor} = \left(\frac{\frac{2}{3} \mu_2 + \frac{1}{3} \mu_1}{\frac{2}{3} \mu_2 + \frac{1}{3} \mu_1} \right) \rho_2 \quad (7)$$

For a low viscosity liquid drop falling in high viscosity liquid field, the correction factor of 1.6 had been determined for a fully circulating drop. If the viscosities of the two fields are equal the correction factor of 1.6 may be considered.⁶ Very often, infinite

of low viscosity of the liquid drop, the Stokes law is applied because of the rigidity of the surface of the drop due to the presence of unavoidable impurities.⁹

Velocity pattern in drops falling through glycerine solution had been studied by Garner and Raycock¹⁰ and their observations revealed that no circulation was possible until the fall velocity exceeded 0.8 cm/sec.

due to mobility of the interface, the velocity gradients present in the liquid are smaller than those in the case of solid interface. With the same driving force (gravity), the velocity of steady fall of a liquid drop should be greater than the velocity of fall of a solid sphere.⁷

The liquid on the surface of the drop moves at a velocity

$$(U_0)_{r=a} = U_0 \sin \theta \quad (8)$$

Where U_0 is the magnitude of liquid velocity at the drop equator and $U_0 \sin \theta$ is the velocity on the surface of the drop at an angle θ from the drop equator. Again,

$$U_0 = \frac{\mu_0}{\frac{\mu_0}{2}} = \frac{\eta}{\mu_0 + \mu_p} \quad (9)$$

Where $\mu_0 \gg \mu_p$, the velocity on the surface is small and limit becomes zero in the case of solid surface.

3.3.3. Diffusional flux on the drop surface

Levich deduced the diffusional flux to the surface of a drop, falling in a liquid where $n_0 \gg 1$. The density of the liquid in the drop was considered to be higher than that of the liquid medium. The total flux I , on the surface of the drop was found to be:

$$I = 4 \pi (C_0 - C) \sqrt{\frac{D}{\pi}} \left(\frac{R_0 n_0}{\gamma} \right)^{1/2} \quad (10)$$

If $n_0 > 1$ and certain diffusion boundary layer exists on the surface of the droplet, its thickness δ can be found out from the relation:

$$n_0 \frac{D}{r} \approx D \frac{C}{\delta^2} \quad (11)$$

For $n_0 > 1$, the velocity of the liquid u_0 on the surface of the drop will be equal to the velocity of the falling drop. Hence by putting $u_0 = 0$ in equation(11) and by rearranging, the final form will be:

$$\delta = \sqrt{\frac{D}{\pi}} \quad (12)$$

The general equation for diffusional flux on the surface of the drop is $I = \frac{D}{\delta} (C_0 - C) A$ (13)

Substituting equation (12) in (13) and rearranging, the total flux on the drop surface in the case when $n_0 > 1$ will be:

$$I = 4 \pi r^2 (C_0 - C) \left(\frac{D}{\pi} \right)^{1/2} \quad (14)$$

The above equation is not valid for very high Reynolds number.⁷

3.1.3. Mass Transfer Model:

The mass transfer between a single sphere and surrounding fluid is usually divided into three parts.¹¹

- (a) Transfer within the sphere.
- (b) Transfer through the interfacial phase
- (c) Transfer outside the sphere.

The conditions which are necessary to be fulfilled prior to the studies are:

- (a) Interfacial tension of the liquid drop should be high in order to maintain the shape of the drop.
- (b) The velocity of the continuous phase should be uniform in the region surrounding the drop.
- (c) Fluids are dilute and binary diffusion equations are applicable.
- (d) Heat generated by solution of transferring species are small.
- (e) Pressure and temperature gradient is negligible.

When the drop behaves as a rigid sphere, the transfer rate can be determined from the molecular diffusivity, whereas more enhanced value other than molecular diffusivity has to be considered when the drops

are in the state of internal motion. The continuous phase mass-transfer resistance follows closely that reported for solid spheres in the circulating regime where as the effective diffusivity within the drop is a constant multiple of the molecular diffusivity.¹²

It is possible in some cases that the mass-transfer resistance is in the drop phase. The overall transfer rate will be controlled by the extraction mechanism inside the drop and to a $\frac{1}{2}$ extent by the hydrodynamics of the system. Both molecular and convective diffusivity may influence the transfer rate in the dispersed phase. Extraction efficiency can be expressed in terms of Froese's equation.¹³

$$E = 1 - \frac{E}{E_{\infty}} = \frac{E}{E_{\infty}} \left(1 - \frac{1}{E_{\infty}} \exp \left(-4 + \frac{2}{3} \frac{D_p^2}{D^2} \right) \right) \quad (14)$$

E = fraction extracted (dimensionless).

The circulation model of Fromig and Brink¹⁴ is valid when the relative motion of the drops induces circulation. Turbulence of high intensity in the continuous phase may cause turbulent movement inside the drop. Handlos and Baron¹⁵ proposed the model for mass-transfer under the above mentioned situation. The results from the series of experiment indicated that they do not agree with the above model. So one experimental factor β has been introduced in the equation. β when multiplied

with molecular diffusivity becomes more or less the effective diffusivity.¹⁵

Gerner and Gownlock¹⁶ studied the effect that droplet oscillation had on the continuous phase resistance. Lee and Hartner¹⁶ suggested a model for vigorously oscillating single liquid drop, moving in a liquid field with the concept of interfacial stretch and internal droplet mixing. To predict the initial none thickness for a spherical drop with uniform internal concentration of solute, two film theory ^{been}applied, the liquid film thickness is predicted by using the spherical correlation of Gerner and Gownlock which is:

$$R_{eq} = 0.5 R_{eq}^{\frac{1}{2}} R_{eq}^{\frac{1}{2}} \quad (18)$$

To predict the inside film thickness, the penetration theory is used with contact time equal to the time for one oscillation cycle. This contact time was chosen as a result of photographic study of the pattern of movement inside a falling oscillating drop. During each time, the droplet underwent a period of oscillation, the interior of the drop was violently mixed, so the interface will be renewed during each droplet oscillation. Hence,

$$R_p = .46 (R_p W)^{\frac{1}{2}} \text{ cm/sec.} \quad (19)$$

W = frequency of oscillation in $\text{rads}^{-1}/\text{sec.}$

since the overall mass transfer coefficient is

$$\frac{1}{R_0^2} = \frac{1}{R_0^2} + \frac{2}{R_0} \quad \text{where } \alpha = \left(\frac{\rho_A - \rho_B}{\rho_A + \rho_B} \right) \frac{\text{drop shape}}{\text{cave shape}} \quad (27)$$

In Hsu and Kintner model, the oscillation has been considered as surface life time and the area change resulting from one oscillation has been assumed constant. Anglin and Lightfoot¹⁷ modified the Hsu and Kintner concept and studied the penetration theory for surface stretch applied to oscillating droplets in the Reynolds number ranges between 100-2000. Further modification and studies in the Reynolds number range between 10-100 was conducted by ~~Wang~~¹⁸ and Lightfoot¹⁸ and they observed that the distortion of drop changes the Nusselt number by about 20%. All these studies have been made with liquids of low density and viscosity.

It has been known for quite sometime that the composition of the liquid metal at the beach is very much different as compared to the metal at the hearth. Earlier workers tacitly assumed that the site for slag-metal reaction was the interface between the slag and the pool of metal. Therefore, they essentially simulated the slag and metal pool in the laboratory and studied the reaction kinetics. However, from heattransfer considerations, there was no reason¹⁹ to ignore the chemical reaction while the metal droplets are passing through the slag. As a matter of fact, some recent studies⁽²⁰⁾⁽²¹⁾ have shown

that the desulfurization takes place primarily while droplets fall through the slag layer. When this work was undertaken no investigation in this direction could be located in the literature.

The situation is very complex involving thousands of droplets of different sizes and specific chemical and physical conditions. A clear understanding of the process may emerge through controlled drop studies. The knowledge gained from the performances of individual large drops may not be immediately applied to the complex operation. However, this is expected to be of considerable help to understand the mass-transfer situation. It is in this context, the decision was taken to examine the phenomena exhibited by single drop moving through the viscous liquid layer with the help of a solid model.

2. PLAN AND OUTLINE OF THE WORK

The difficulties of handling molten slag and metal at high temperatures can be eliminated with the help of room temperature systems in which the densities and viscosities of the two phases should bear some resemblance to the actual process. Different techniques had been adopted to study the mass-transfer to or from the droplets and the bubbles. Constant volume experimental technique as adopted by Calderbank⁽²²⁾ and Cochrane⁽²³⁾ to study the mass-transfer from bubbles can be applied to droplets also. Sedimentation technique for instantaneous measurement of exchange rate of the solute on freely suspended single drop had helped in studying the exchange process without affecting the hydrodynamics of the system⁽²²⁾. Calderbank⁽²⁴⁾ and Cochrane⁽²⁵⁾ observed that mercury drops formed one drop diameter above the continuous phase were not distorted while passing through the liquid surface.

In this study, mercury drops were formed above the surface of the aqueous phase in conformity with the actual plant furnace condition and the (i) mass transfer from the droplets while passing through the aqueous phase (ii) Diffusion co-efficient of the solute in the aqueous phase (iii) Velocity and the residence time of the droplets in the aqueous phase were determined. The dropping rate was

is assumed that only one drop at a time passed through the aqueous phase.

2.1 Approximation of Mass-transfer Co-efficients.

In the experiments, mercury droplets were used to simulate the metal phase and water with its viscosity adjusted with glycerol was equivalent to the slag phase. Typical reactions which are conveniently used for studying mass transfer between slag and metal without production of gas at the interface are



square brackets indicate the metal phase and round brackets the aqueous phase.

Swenson and Richardson⁽¹⁰⁾ studied the mass transfer across interface agitated by bubbles in both systems represented by equations (13)(14) under equilibrium and metal saturated conditions.

For the purpose of estimation from the drop-size, equation (12) can be favourably used. In the analysis of different droplet sizes were passed through aqueous phase of different ferrous ion and glycerol concentrations in the series of experiments it was planned to verify whether aqueous control condition existed in the system

or not.

The small emulsion pool formed at the bottom of the apparatus was kept separated from aqueous solution in order to avoid any reaction between the two liquids.

3.2 Diffusion Coefficient of Fe^{3+} ion.

During the course of experiment, the concentration of ferric ion in the aqueous phase is supposed to be reduced, hence the diffusion coefficient of ferric ion is expected to vary. So, it is essential to determine the diffusion co-efficient of ferric ion as a function of concentrations in the aqueous phase. Diffusion co-efficient of ferric ion at various concentrations under different glycerol content similar to experimental conditions for mass transfer study were carried out by Polarographic technique.

3.3 Velocity and residence time.

Knowledge of velocity and residence time for the droplets in the aqueous phase is important in order to determine the hydrodynamics and the mass transfer results. Photographic techniques were adopted for the measurements of terminal velocity and the residence time of the droplets in the aqueous phase.

3. EXPERIMENTAL

The aqueous solutions used for studying the reaction in equation (10) consisted of FeCl_3 at various concentrations ranging from 10-70 m-moles/liter and A.R. grade glycerol between 15-70 wt percent for adjusting the viscosities of the aqueous phase. The pH of all the solutions were adjusted to 1.4 by adding A.R. grade HCl before every experiment. All aqueous solutions were deaerated prior to use by passing purified nitrogen for 2 hours.

The amalgams were prepared from triple distilled mercury and iodine of 99.999 percent purity.

3.1 Analytical techniques.

Polarographic techniques were used for measuring the concentrations of indic ions and the diffusion co-efficients of ferric ions in the aqueous phase. The apparatus consists of a mercury reservoir fitted with a capillary tube at the bottom and a calomel electrode in one branch of T tube and the other branch is the sample container separated by porous disc. Mercury drops are the dropping electrode formed from the capillary of 0.01- .05 mm bore under constant pressure and time interval. Calomel electrode has been provided to eliminate the possibility of unknown or nonreproducible anode potential, hence it acts as reference electrode. In polarography actually

the current vs. E_{app} plot is recorded (26)

A concentration gradient is established between the dropping electrode surface and the bulk solution. At equilibrium, the rate of discharge of ions by current is equal to the rate of diffusion to the electrode surface. For relatively small values of current, the concentration overpotential is small and as the applied E_{app} is increased beyond the decomposition potential, the current exhibits the normal sigmoidal stage is reached at which the concentration overpotential increases rapidly and the current reaches a limiting value, hence this is the maximum rate at which particular ion can be discharged under the given experimental condition. As the concentration of the bulk solution increases, the limiting current also increases. The galvanometer is unable to follow the periodic growth and fall of the current of each individual drop, so the raw recorded waves are observed. This is measuring the diffusion current, the average of the galvanometer oscillation is to be considered (27).

In order to obtain true diffusion current of a substance, a correction must be made for the residual current. The most reliable method for making this correction is to estimate in a separate polarogram the residual current of the supporting electrolyte alone. The value of the residual current at the particular half wave potential

© 1999 Blackwell Science Ltd
Journal of Internal Medicine 245: 373–382



FIG. 4. CORRECTION TECHNIQUE FOR THE DETERMINATION OF CONCENTRATION AND DIFFUSION COEFFICIENT USING POLAROGRAPHY

level of the corresponding element is subtracted from the total observed current⁽¹²⁷⁾. Fig. 1 indicates the corresponding techniques for the determination of diffusion current. Correction technique has been adopted for the determination of concentration and diffusion coefficients.

All the electroactive materials have their half wave potential. This is the potential at the point of current-voltage curve, half the distance between the residual current and the final limiting current. Hence it is customary to measure diffusion current at the half wave potential level. In the case of D_2 , the value of half wave potential changes with pH. At pH 3.5-4, half wave potential is ~ 0.60 volts⁽¹²⁸⁾ and ~ 0.64 volts for Ferric ion at pH⁽¹²⁹⁾. For the determination of concentration of In in the aqueous phase, the pH of the solution has to be maintained at 1.4 and with backing electrolyte, the resultant pH was within 3.5-4.

Before each experiment, the solution is deaerated by passing purified nitrogen for 10-15 minutes.

4. Description of the apparatus.

The apparatus used for monotransfer study is shown in Fig. 2. It is a 15 cm long tube of 4 cm diameter resting on a container for storing the used amalgam. Suitable siphoning arrangement has been provided to draw out the amalgam from the column at proper interval.

Since the Hg-In amalgam gets oxidized very easily in air, suitable arrangement has been made to maintain nitrogen atmosphere on the liquid column. Since the desaturation of the solution is required before each experiment, suitable provision has been made for this purpose. There are three openings at the top of the apparatus. The center hole for dropping amalgam and the other two are for sampling and thermometer point. The whole apparatus is completely air tight and immersed in constant temperature bath.

The auxiliary part of the apparatus is the amalgam preparation and dropping unit. The amalgam is stored on separate column and drops into the dropping column after certain interval of time in order to maintain more or less constant level in it. The height of the amalgam column from the top level of the amalgam pool to the tip of the capillary was maintained at 30 cm. Provisions are there to maintain nitrogen atmosphere on the amalgam storage and in the dropping unit.

The whole apparatus is made up by Pyrex glass and suitable ground glass joints has been used for sealing purposes.

4.1 Membringer's Membrane

Before starting the experiment, a layer of "Vulca-Sealantone" of 2 mm thickness was made at the bottom of the apparatus in order to separate the amalgam

pool from the aqueous solution. Tetra bromo ethane is of density 2.4, reacts neither with aqueous phase nor with the analgesic. Hence, the measurement only from the drop-lets can be studied.

In all the experiments 500 cc of aqueous solution containing different proportions of glycerol and PEG, after adjusting the pH to 1.4 was poured slowly on the top of the tetra bromo ethane. The height of the aqueous column was 10 cm in all the cases. The solution was thoroughly deaerated by passing purified nitrogen for two hours.

Some experiments were conducted at 21-22°C in the present apparatus, where appreciable amount of transfer could not be detected. With a column height of 40 cm, sufficient amount of transfer was recorded with 60 cc aqueous solution at a temperature of 22-23°C. Since it was difficult to fulfill the experimental requirements in the tall column, experiments at higher temperature was tried. Hence all the experiments were conducted at 30°C. It was possible to control the temperature of the constant temperature bath upto $\pm 1^{\circ}\text{C}$.

Capillaries of 1 mm and 0.8 mm inside diameter were used for dropping analgesic. All the capillary tips were polished and cleaned thoroughly before use.

Amalgam was prepared by pouring the weighed amount of mercury on the ladle under nitrogen atmosphere, blowing by purified nitrogen into the stored amalgam for 1-2 minutes was preferred to ensure thorough mixing. No scale formation on the surface of amalgam storage was observed. Storage column and the dropping unit remained under nitrogen atmosphere through out the experiment.

As soon as the preparation of amalgam was over, certain amount of amalgam was drawn out from storage to the dropping unit, deaerated the capillary and the connecting rubber hose. This amalgam was stored separately and subtracted from the total amount in order to calculate the actual amount of amalgam used in each experiment. Before starting the experiments, 5-10 drops of amalgam were collected in the weighing bottles under identical condition in order to determine the equivalent diameter of the droplets. Identical dropping rate could not be maintained in all the experiments but in individual experiments some drop rate from the beginning to the end was maintained. Drop rate varied between 100-200 per minute in the case of small capillary and 100-300 per minute for the bigger one. The above mentioned dropping rate was sufficient to observe the passage of a single droplet through the liquid column at a time. The amount of amalgam passed through the solution varied between 1000-1500 gms in the case of small

capillary and 1800 - 2000 ga for the big one. The capillary ports with small capillary contained from 20-30 ml solution and with big capillary from 80 - 110 ml.

Subramanian and Richardson⁽²⁶⁾ work indicated that the initial concentration of In in the amalgam had no effect on the observed rates of anastropher. The capillary cells were tried with different In concentrations and the same results were obtained. Hence it was decided to conduct all the experiments with In concentration of 0.001.

Viscosity of the liquid phase ~~was varied~~ from 0.78 cp to 11.78 cp and ferric ion concentration from 10-78 m. moles per liter.

In all the experiments, after passing amalgam through the aqueous solution for certain interval of time, 2 cc of the solution was drawn out through the sampling hole and analyzed polarographically for indium content. The characteristic half wave potential of In^{3+} and Fe^{3+} are widely separated. To prevent Fe^{3+} from oxidizing the dropping mercury electrode, 2M potassium chloride containing 50 ga/liter of hydroxy monochloroacetic was used as a backing electrolyte.⁽²⁵⁾ The addition reduced the ferric ion to Fe^{2+} . The diffusion current varied linearly with concentration and was not affected by glycerol content. Correction method as indicated earlier was followed to determine the $\tau^{-1/2}$; diffusion current for indium ion. Again

polarographically determined the diffusion current for ferric ion of a standard indium chloride solution of known concentration in the presence of a backing electrolyte of 1 M HCl/liter. Similarly correction given was adopted in finding out the i_{d0} diffusion current. Then from the relation

$$\frac{C_1}{C_2} = \frac{i_{d1}}{i_{d2}}$$

where C_1 = Concentration of ferric ion in unknown solution
in M. moles/liter. (milli-moles/liter)

C_2 = Concentration of ferric ion in standard solution
of known concentration, in M. moles/liter.

i_{d1} = diffusion current for unknown solution in
microampere.

i_{d2} = Diffusion current for known solution in
micro amp.

the concentration of ferric ion in the aqueous phase was determined. This procedure was adopted in all the samples. By stoichiometry, from the concentration ^{of} ferric ion, the amount of ferric ion consumed after certain interval of time was calculated.

4.3 Diffusion coefficient of ferric ion.

In the mass transfer experiments it was observed that the concentration of ferric ion in the aqueous phase was decreasing, hence the diffusion co-efficient values might also change. $D_{Fe^{3+}}$ values are available only at 30°C. Since all the mass transfer experiments were carried out

at 35°C , as the $D_{\text{Fe}^{3+}}$ values at different concentrations of ferric ion and glycerol were determined by polarographic technique at 35°C .

In the course of experiments, concentrations of ferric ion were varied between 0.05- 01.5 m. moles/liter in water, 10.5 - 01.5 in water + 50% wt glycerol and 10.5 - 04 m. moles per liter in water + 75 wt per cent glycerol ^{medium}. The backing electrolyte ⁽²⁰⁾ was 0.05M per liter sodium oxalate and .005% gelatine as mercuric suppressor. It was observed that .005% gelatine was sufficient for water and water + 50 wt % glycerol medium but in case of 75 wt % solution, the gelatine addition was increased to .01 % . The pH of the solution was adjusted to 4 by adding acetic acid before each experiment.

Known volume of solution was taken in the sample holder and deaerated for 15 minutes before the start of the experiment. Temperature control was $35^{\circ}\text{C} \pm .5^{\circ}\text{C}$. The drop time and weight of mercury passed per second were determined. Cuvette method was adopted in determining the mV diffusion current for each sample from the Polarograms. From the law governing the condition of diffusion at a dropping mercury electrode and periodic growth and fall of the droplets, theoretical equation for diffusion current as developed by Ilkovic ⁽²¹⁾

$$I_d = 607 \pi D_{\text{Fe}^{3+}}^{1/2} C m^{1/2} t^{3/4} \quad (22)$$

Δd = diffusion current in micro amperes during the life of the drop.

F = number of Faraday electricity required per mole of the electrode reaction.

c = concentration in millimoles per liter.

m = rate of flow of mercury in mg/sec.

τ = drop time in sec.

$D_{\text{Fe}^{3+}}$ = diffusion co-efficient of ferric ion in $\text{cm}^2/\text{sec.}$

From eqn. (20).

$$D_{\text{Fe}^{3+}}^{\frac{1}{2}} = \frac{l_d}{407 F \cdot c \cdot \pi^{1/2} \tau^{1/2}} \quad (21)$$

$D_{\text{Fe}^{3+}}$ for all the solution are calculated and reported in table no.3. The plot $D_{\text{Fe}^{3+}}$ vs. concentration is shown in fig. 4 which helped in determining diffusion co-efficient at any concentration within the experimental range. The reproducibility of diffusion current values were checked and these were within $\pm 1\%$.

4.3 Velocity and Residence Time Determination.

The terminal velocity and the residence time of the droplets of different sizes in the different aqueous media, similar to microelectrode experimental conditions were determined by photographic means. Several photographic exposures at regular time intervals of a drop falling through the aqueous phase were taken by using EHDENAF- Type 1881-22 (General Radio Company) in a darkened room. For

bigger drops 3000 ^{Optical} ~~Fig. 8~~ and for the smaller ones 4000 ^{Fig. 8} ~~Fig. 8~~.
Settings were used. The photographs are shown in
Figs. 8a,b. The photographic studies revealed that the
small drops were reaching their terminal velocities with-
in 1-1.5 cm travel distance from the liquid surface, the
corresponding travel distance was 3-3.5 cm in the case of
big drops. Residence time and the terminal velocities
were calculated from drop intervals and the strokoscopes
data.
Values for all the cases are reported in Table 1.2

Movie Camera was used in determining the
change of shapes of the droplets when were taking place
during its passage through the aqueous phase by using
strokoscopes. It was possible to observe the changes in
shape at different positions of the liquid column but
due to certain limitations, complete shape changes could
not be recorded hence shapes could not be measured.

A few interesting movie photographs are shown in Fig. 8.

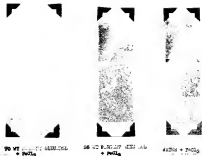


Fig. 3a, b - Thermal velocity and resistance time determination by photographic technique.

800 8100 0000000



Fig. 8a,b vertical velocity and resonance line determination by photographic technique.



Fig. 4 - Shows the condensation and changes in shape also during its passage through the system (glass) (water + HCl).

TABLE III

Properties of the acetals tested and other experimental data are given in Table Ia and Ib.

TABLE III

Run No.	Acetal prepared	Boiling point, °C. at 1 mm. Hg.	Viscosity, cP. at 25°C.	Density, g./ml. at 25°C.
1	70	88	1.75	1.176
2	70	70	11.75	1.18
3	70	50	11.75	1.17
4	70	85	11.75	1.176
5	water	88	.754	1
6	85	85	2.65	1.09
7	85	85	2.65	1.09
8	water	85	.758	1
9	water	85	.758	1

* Viscosity and density data taken from Handbook of Chemistry and Physics, Forty-third edition.

Table 1.2

Year	1950-1954	1955-1959	1960-1964	1965-1969	1970-1974
1	.189	.185	.188.1	.17.02	.185
2	.189	.180	.1770	.17.02	.185
3	.189	.188	.179.8	.17.02	.175
4	.189	.186	.1835.7	.17.02	.185
5	.187	.188	.1834	.70.8	.187
6	.189	.188	.1178	.83.8	.188
7	.184	.188	.1880.8	.73.07	.188
8	.188	.185	.1834.8	.73.80	.187
9	.188	.188	.1888	.70.8	.187

results from mass transfer experiments are shown
in table II

TABLE II

EXP. NO.	CONC. OF Fe^{3+} in aqueous phase in m. moles per liter	INITIAL FORMIC ACID CONC. IN ORG. PHASE IN MOLES PER LITER $(Fe^{3+})_{t_0}$	$\frac{(Fe^{3+})_t}{(Fe^{3+})_{t_0}}$	TIME IN SEC.
1	0.18	25	0.6028	3000
	0.276	25	0.6069	6000
	0.36	25	0.6093	9000
	0.454	25	0.6010	12000
	0.55	25	0.6033	15000
2	1.0456	75	0.603	3000
	1.4126	75	0.603	10000
	1.819	75	0.603	15000
	2.1787	75	0.603	18000
	2.528	75	0.603	21000
3	0.368	10	0.603, 0.604	18000 12000
	0.463	10	0.603	15000
	0.56	10	0.603	12000
	0.66	10	0.603	9000
	0.768	10	0.603	6000
4	1.1187	25	0.603	18000
	1.4003	25	0.603	15000
	2.808	25	0.603	9000
	4.1047	25	0.6074	13800
	4.8117	25	0.6108	16300
5	0.668	25	0.603	12000
	1.730	25	0.603	9000
	2.608	25	0.603	13800
	3.503	25	0.6000	16300
	4.408	25	0.618	1900
6	1.8008	25	0.603	9000
	2.702	25	0.604	12000
	3.6005	25	0.603	15000
	4.503	25	0.603	18000
	5.408	25	0.603	21000
7	2.0008	25	0.603	9000
	3.0008	25	0.603	12000
	4.0015	25	0.603	15000
	5.0015	25	0.603	18000
	6.0015	25	0.603	21000
8	1.8010	25	0.603	9000
	2.8010	25	0.603	12000
	3.8010	25	0.603	15000
	4.8010	25	0.603	18000
	5.8010	25	0.603	21000

Plots of $\log \left(\frac{(Fe^{3+})_t}{(Fe^{3+})_{t_0}} \right)$ vs. time are shown in fig. 3a, 3b

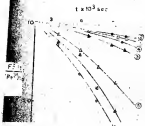


Fig. 5a. RESULTS OBTAINED FROM ANALYSIS OF
 SMALL DROPLETS 1-5, 100-150 μ IN
 A CARBON MONOXIDE PHASE - 75-100
 PLOTTER 1-10, 100-150 μ .
 INDICATE THE CRYSTAL GROWTH
 WHICH IS ASSUMED TO BE 1-100-150

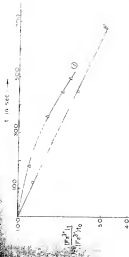


FIG. 3b RESULTS OBTAINED FROM EQUATION (1) FOR $\alpha = 0.01$ AND $\beta = 0.01$ FOR $\gamma = 0.01$ IN AN INFINITE MEDIUM. THE DATA WERE OBTAINED FROM THE RESULTS OF EQUATION (1), USING $\alpha = 0.01$ AND $\beta = 0.01$ FOR $\gamma = 0.01$ IN AN INFINITE MEDIUM. THE RESULTS WERE OBTAINED FROM EQUATION (1).

Photographic results for the diffusion coefficients of ferric ion in the different aqueous media are in Table No. III a,b,c.

TABLE III a

In water at 30°C \pm .5°C

Fe- No.	Conc. of Fe ³⁺ in 300 ^{ml} water per liter.	Diffusion co-efficient in cm ² /sec.
1	0.25	7.0000×10^{-6}
2	10.50	6.9400×10^{-6}
3	10.75	6.8000×10^{-6}
4	20.00	6.5400×10^{-6}
5	31.25	4.2000×10^{-6}

TABLE III b

In 25 wt% glycerol + water at 30°C \pm .5

1	10.5	
2	10.75	2.7000×10^{-6}
3	20.00	2.6175×10^{-6}
4	31.25	1.6000×10^{-6}

TABLE III c

In 70 wt percent glycerol at 30°C \pm .5

1	10.5	6.4100×10^{-7}
2	10.75	6.4000×10^{-7}
3	20.00	7.8000×10^{-7}
4	31.25	4.3040×10^{-7}
5	64.00	1.7000×10^{-7}

Values of Diffusion co-efficient vs concentrations of ferric ion from Table III a,b,c have been plotted and shown in Fig.45

Diffusion coefficient

70 wt% H_2SO_4

70 wt% H_2SO_4

Fig. 4. Diffusion of ferric ion at 35°C. in 70 wt% H_2SO_4 and ferric ion in 70 wt% H_2SO_4 .

6. Discussion of the results

6.1 Kinetic steps

the reaction being studied is



the kinetic steps are

- 1) transport of Fe^{2+} ions to the interface from the aqueous phase (bulk)
- 2) transport of In from the bulk amalgam to the interface
- 3) reaction at the interface (eqn.14).
- 4) transport of In^{2+} from the interface to the aqueous phase
- 5) transport of Fe^{3+} from the interface to the aqueous phase.

The chemical reaction at the interface (step 3) is expected to be very fast because it essentially involves electron exchange amongst atoms and simple ions. Dubrovskii and Richardson²⁰ also found it to be very fast. Hence step(3) is not at all expected to be rate controlling.

If the process is solely transport controlled, then chemical equilibrium amongst the various species may be assumed. The equilibrium relationship for the reaction in equation (14) is as follows,

$$K = \frac{(\text{In}^{2+})_{\text{I}} (\text{Fe}^{3+})_{\text{I}}^2}{(\text{In})_{\text{I}} (\text{Fe}^{2+})_{\text{I}}^2} = \text{calc}^{2.0} \quad (15)$$

where K is the equilibrium constant for the reaction (49). The brackets indicate the concentration of the species in the aqueous and metal phases and the suffix 1 indicates the concentration of the species at the interface in gram mole per c.c.

Because In^{3+} and Fe^{2+} are moving out from the interface to aqueous phase, $(\text{In}^{3+})_1$ and $(\text{Fe}^{2+})_1$ must be greater than $(\text{In}^{3+})_{\text{bulk}}$ and $(\text{Fe}^{2+})_{\text{bulk}}$ respectively and hence must be greater than zero as soon as the experiment has commenced. Since K is very large, and the numerator in eqn. (50) cannot be infinity, therefore the denominator must be tending to zero. This is possible provided either $(\text{In}^{3+})_1 / \gamma_{\text{In}^{3+}}^2$ tends to zero.

If the rate of transport of Fe^{2+} is less than that of In in the amalgam, then $(\text{Fe}^{2+})_1$ would tend to zero and $(\text{In}^{3+})_1$ would be close to $(\text{In}^{3+})_{\text{bulk}}$. For rate calculations, we may take $(\text{Fe}^{2+})_1 = 0$ without any significant error. The question is under such circumstances which transport step is rate-controlling? Step (3) has already been assumed too fast. As regards, transport of Fe^{2+} and In^{3+} [Steps (4) and (5)] are concerned, it may be stated that they are able to adjust themselves to match the rate of transport of Fe^{2+} . The adjustment would be achieved because the values of $(\text{Fe}^{2+})_1$ and $(\text{In}^{3+})_1$ can go up to their respective limits of solubility. Even if the solubility limits are reached, removal of Fe^{2+} and In^{3+} from the interface is possible by precipitation from solution. In this investigation, no precipitation effect was found. Hence the values of $(\text{Fe}^{2+})_1$ and $(\text{In}^{3+})_1$ were below their respective solubility limits. Hence

It can be concluded that step (4) and (5) would adjust themselves to fulfil the rate of step (1) and hence step (2) would be the rate-controlling step with $(\text{Fe}^{3+})_1 \approx 0$. This has been called "aqueous control" by Gunnarsson and Westgren²⁵.

A reverse situation can also be possible, where the rate of transport of I^- in the emulsion is much slower as compared to that of Fe^{3+} . Following the arguments given above, it can be similarly shown that transport of I^- in the emulsion would be rate-controlling with $(\text{I}^-)_1 \approx 0$. This has been termed as "metal control" by Gunnarsson and Westgren²⁵.

A third possibility is mixed-control of step (1) and (2) where the values of both $(\text{I}^-)_1$ and $(\text{Fe}^{3+})_1$ tend to zero.

In this investigation, the aim has been to study the aqueous control only and in order to achieve this the concentration of iodine in the emulsion was kept high.

3. Determination of mass-transfer coefficient from experimental data.

Mass-transfer coefficients have been calculated from the change of concentration of iodine in the aqueous phase. This section presents the various equations that correlated experimental variables with mass-transfer coefficients.

Case I : Transport of Fe^{3+} in aqueous solution rate-controlling

If n is number of droplets per unit time on a per sec, and the residence time of one droplet in aqueous column is T sec, then the number of droplets in the bath at any moment would be equal to nT .

Since the transport of Fe^{2+} is rate controlling, and $(\text{Fe}^{2+})_d = 0$, hence

$$I_{\text{Fe}^{2+}} = k_{\text{Fe}^{2+}} S + C_{\text{Fe}^{2+}} S \quad (10)$$

where S is total surface of (Fe^{2+}) in the aqueous solution

$$\pi r^2 d^3 \frac{4}{3} \pi \frac{C_{\text{Fe}^{2+}}}{V_a} = - V_a \frac{dC_{\text{Fe}^{2+}}}{dt} \quad (11)$$

where $I_{\text{Fe}^{2+}}$ = mass flow of ferrous ion

d = diameter of the droplets in cm,

$k_{\text{Fe}^{2+}}$ = mass transfer coefficient for ferrous ion in cm/sec,

$C_{\text{Fe}^{2+}}$ = concentration of ferrous ion in the aqueous phase whose transfer was rate controlling, in g. moles/liter

V_a = volume of the aqueous phase in c.c.

By rearrangement and integrating within the limits it could be expressed as

$$\log \frac{(\text{Fe}^{2+})_d}{(\text{Fe}^{2+})_{t_0}} = - K' t \quad (12)$$

where subscript t_0 and t denote the concentration on initial and final times and $K' =$

$$\frac{\pi r^2 d^3 \frac{4}{3} \pi \frac{C_{\text{Fe}^{2+}}}{V_a}}{V_a \frac{dC_{\text{Fe}^{2+}}}{dt}}$$

From the plots in figure 5a, 5b, K' being the slope and $k_{\text{Fe}^{2+}}$ was calculated from the experimental values of t_0, d, r and as mentioned in the experimental chapter. The concentration of Fe^{2+} in the aqueous phase at different interval of time were determined polarographically and the concentrations of ferric ion were calculated from stoichiometry as in eqn (10) (for details refer to chapter 4.)

Integration of acceleration ratio of iodine ion can be plotted against the weight of sodium peroxide per unit time instead of the case as shown in \overline{D}_1 , \overline{S}_1 , \overline{S}_2 . The total weight of analyte passed during the course of the experiment for the period of 1 sec will be

$$w = \int_0^1 d^3t \times 10.8 \times 10^3 \quad (26)$$

Where w is the weight of Na_2O_2 in gm.

From eqn. (26)

$$-k^2t = - \frac{.0704 \overline{D}_1^2 \overline{S}_1^2}{2.303 \overline{V}_1} t \quad (27)$$

Substituting eqn. (26) in (27) and rearrangement

$$-k^2t = - \frac{.104 \overline{V} \overline{D}_1^2 \overline{S}_1^2}{2 \overline{V}_1} t \quad (28)$$

Hence eqn. (25) is modified and expressed as

$$\log \frac{(\overline{P}^{2+})_{\text{final}}}{(\overline{P}^{2+})_{\text{initial}}} = - \frac{.104 \overline{V} \overline{D}_1^2 \overline{S}_1^2}{2 \overline{V}_1} t \quad (29)$$

Plot $\log \frac{(\overline{P}^{2+})_{\text{final}}}{(\overline{P}^{2+})_{\text{initial}}}$ vs t should be straight line and from the slope $\overline{D}_1 \overline{S}_1$ could be calculated when the other terms like d , \overline{V} & \overline{V}_1 etc. were experimentally determined.

Case 2: Transport of I_2 in the analyte rate controlling.

The mass transfer coefficient for iodine $k_1(\overline{D}_1)$ could be calculated similarly by mass balance as before. The concentration of iodine in the drop phase would be constant in each experiment, since the transport of iodine is rate controlling and $[\text{I}_2]_1 \approx 0$ hence

$$\frac{d\ln}{dt} = K \frac{[D]_t}{[D]_{t_0}} \quad (20)$$

the iron balance equation expressed as

$$\int_0^t dt \frac{d[D]_t}{[D]_t} = \frac{[D]_t}{[D]_{t_0}} = - \frac{V_d}{V_s} \ln \frac{[D]_t}{[D]_{t_0}} \quad (21)$$

where $K_{[D]}$ = mass transfer co-efficient for indium in drop phase,

$C_{[D]}$ = conc. of In in the aqueous ferric, the complex
in weight percent,

V_d = volume of the drop in c.c.

t = time in sec.

δ = diameter of the drop in cm.

By rearrangement and integrating within the limits

$$\log \frac{[D]_t}{[D]_{t_0}} = -K^* t \quad (22)$$

where the subscripts t_0 , t denotes the concentrations in

initial and final time and $K^* = \frac{V_d K_{[D]} [C_{[D]}]}{V_s \pi \delta^2}$

from the plot $\log \frac{[D]_t}{[D]_{t_0}}$ vs t , the slope is K^* , hence $K_{[D]}$ can be calculated.

Concentration of indigo after an interval of time can be obtained either by analyzing the used analyzer or by analyzing its concentration in the aqueous phase by polarography.

C. Nature of experimental data

The results with reaction in eqn. (20) with 0.08% indium in analyzer and ferric ion varying between 10-75a. value per liter in the aqueous phase (1.75-11.75 cp) are plotted in $\log = \frac{[D]_t}{[D]_{t_0}}$ where $\log \frac{[D]_t}{[D]_{t_0}}$ are shown as function of time.

Table 4

the differences, values calculated from Fig. 3a,
to by computer

Exp. type	Δp_{exp}	Δp_{calc}	Δp_{calc}	Δp_{calc}	Δp_{calc}
to	in m. sec.	in m. sec.	in m. sec.	in m. sec.	in m. sec.
1st exp. points					
exp. error					
1	24.5455	4.78×10^{-7}	1.18×10^{-6}	17.30	
	24.245	4.53×10^{-7}	1.54×10^{-6}	21.80	
	20.8935	4.84×10^{-7}	1.49×10^{-6}	20.80	15.577
	22.610	4.87×10^{-7}	1.80×10^{-6}	22.80	
	22.505	4.70×10^{-7}	1.80×10^{-6}	27.45	
2	"	1.58×10^{-7}	1.04×10^{-6}	29.4	29.4
	6.480	7.48×10^{-7}	2.13×10^{-6}	24.7	
3	6.898	7.60×10^{-7}	2.00×10^{-6}	24.9	28.02
	8.428	7.87×10^{-7}	2.34×10^{-6}	44.8	
	8.542	7.87×10^{-7}	4.37×10^{-6}	44.1	
4	26.474	4.77×10^{-7}	1.80×10^{-6}	27.54	
	22.68	4.50×10^{-7}	1.70×10^{-6}	24.80	
	22.6825	4.49×10^{-7}	2.24×10^{-6}	21.80	27.86
	21.6820	4.48×10^{-7}	2.44×10^{-6}	27.20	
	20.8775	4.48×10^{-6}	1.24×10^{-1}	29.80	
	18.80	4.48×10^{-6}	1.80×10^{-1}	44.00	
5	10.888	4.48×10^{-6}	1.70×10^{-1}	64.80	61.09
	10.87	7.00×10^{-6}	1.80×10^{-1}	78.80	
	22.5425	2.42×10^{-6}	4.42×10^{-2}	44.70	
	22.7375	2.42×10^{-6}	4.12×10^{-2}	48.80	
6	27.8175	2.42×10^{-6}	4.42×10^{-2}	64.30	62.27
	24.8975	2.12×10^{-6}	10.42×10^{-2}	62.20	
	22.825	2.42×10^{-6}	4.27×10^{-2}	44.80	
	22.83	2.42×10^{-6}	10.12×10^{-2}	62.24	
7	27.8925	2.42×10^{-6}	1.12×10^{-2}	72.64	69.14
	28.8975	2.42×10^{-6}	1.12×10^{-2}	77.10	
8	"	4.42×10^{-6}	1.82×10^{-1}	62.12	62.12
	22.9725	4.42×10^{-6}	1.82×10^{-1}	61.012	
9	"	4.42×10^{-6}	1.82×10^{-1}	62.12	62.12
	24.2425	4.42×10^{-6}	1.82×10^{-1}	62.52	
	22.8975	4.42×10^{-6}	1.72×10^{-1}	62.402	

The surface mass-transfer co-efficients are given in table- 6.

If the surface tension, pressure, drop size or the concentration of indigo in aq. soln. shall not affect the rate of mass-transfer. In order to verify this, the concentration of indigo was increased by a factor of 5 in two experiments. In one case the rate for 0.001 M. indigo (Compare $k_{p,0}$ values for expt. 30, 5 and 9) and σ_{20} is ignored. In the other case (Compare $k_{p,0}$ values of expt. 30d. with 43), the rate increased by approximately 20 percent. Whereas it may be partly due to some decrease in drop size in expt. 43. Therefore, it may be safely concluded that the influence on rate because of a change in C_{20} is not significant. The little variation may be due to some other surface effect because of higher concentration of indigo in the aq. soln.

$$\text{Further more, according to eqn. (20), } \log \frac{(C_2^{2+})_t}{(C_2^{2+})_{t_0}}$$

should vary linearly with t and should be independent of initial (C_2^{2+}) concentration, provided other factors such as drop size, viscosity etc. are kept constant. At 70 wt percent glycerol and small drop size, several experiments were conducted at ferric ion concentrations of 10, 25 and 75 n. moles. The table (iv) shows the mass transfer co-efficient decreases systematically with increase in concentration. However, it has to be remembered that part of this variation is a result of decrease of diffusion co-efficient with increase in concentration. Fig. 4 shows the variation of diffusion co-efficient of ferric ion with change in concentration in different aqueous medium.

If all other factors remain constant, then K_{ps}/D^2_{ps} should be constant. Table 4 compares K_{ps}/D^2_{ps} and it can be seen that K_{ps}/D^2_{ps} does not vary with v_{tr} but vary systematically for exp. 1-4. Therefore, from this point of view, the experiments 1-4 do not basically violate the Agnew's control condition.

Figures 3a, 3b show that the curves mostly show some systematic deviation from linearity. Computer programming with various orders indicated that second order polynomial gives best fitting with the experimental results. The slopes and the Manchester coefficients at various intervals were calculated by computer and given in table 4. The table shows that K_{ps} increases with time except for experiment 1a, 2 and 3 where K_{ps} remains constant. Again this deviation could be due to variation of D_{ps} with concentration. Therefore K_{ps}/D^2_{ps} should be the real basis for deciding the rate controlling step. As table 4 indicates, variation of D_{ps} alone cannot account for the variation in K_{ps} completely. It is not possible to offer any concrete explanation at this stage, but some concentration dependent factors seem to be playing a role or there may be surface effects.

While comparing the results for experiments 5 and 6, it can be seen that Manchester coefficient values in exp-6 has increased by a factor of 2 than in exp. 5a, 6, though lower terminal velocity and higher residence time has been observed in the latter case. The results in table 4 indicates the variation of diffusion coefficient due to change in Agnew's method

that have contributed to the enhancement of the mass transfer coefficient values. In the case of experiment 7 and 8 where bigger drop size was in the same medium as in exp. 5 and 6, the mass transfer coefficient values are different only by 25 percent, even though the difference coefficient values are very much different. Photographic studies as indicated earlier revealed that the bigger droplets oscillated vigorously during its passage through the aqueous phase and no droplet oscillation was there in the case of smaller one. Since the residence time and terminal velocity in exp. 7 and 8 had not differed much, it may be concluded that the droplet oscillation had influenced the mass transfer coefficient values.

3. Correlation of experimental data.

Reynolds number, drag coefficient, Schmidt number, Sherwood number have been calculated from the data in tables 1a, 1b and using average diffusion and mass transfer coefficient from experimental results. The values are given in table 3.

Experimental drag coefficient values have been plotted against Reynolds number in log scale in fig.7 and compared with solid sphere behaviour. In the case of small drops in high viscosity fluid and in the range of Re below 100 as in the case of experiments 1-4, the deviation from solid sphere line is not much. This is in conformity with the photographic observations that small drops did not oscillate and were behaved like solid spheres. In the case of experiment 5 and 9 with small droplets in water, the slight deviation from solid sphere line is there which indicated ^{oscillation} in the droplet. The point 6,7,8 matches with results of Calderbank²⁴ et al

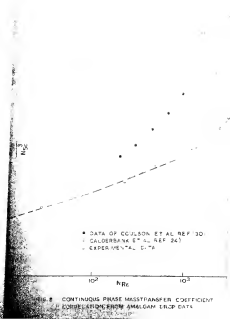
Table 4

Calculated from table No. 1, 1b
and plots No. 1b

Exp. No.	average diffusion coeff. of Fe^{2+} in $\text{cm}^2/\text{sec.}$	average mass transfer coeff. in $\text{cm}/\text{sec.}$	Re_D	C_D	Sh_D	Nu_D
1	4.87×10^{-9}	1.866×10^{-2}	73.0	.971	1.17×10^3	5.16×10^3
2	1.33×10^{-8}	1.64×10^{-2}	73.0	.968	7.98×10^3	1.00×10^4
3	7.73×10^{-9}	2.389×10^{-2}	73.0	.970	1.50×10^3	6.36×10^3
4	4.86×10^{-9}	1.966×10^{-2}	73.0	.968	2.07×10^3	6.16×10^3
5	6.67×10^{-9}	1.441×10^{-1}	1220	.63	1.03×10^3	3.77×10^3
6	2.76×10^{-8}	8.7×10^{-2}	445	.865	8.76×10^3	8.02×10^3
7	3.73×10^{-8}	10.43×10^{-2}	1060	.613	6.56×10^3	10.66×10^3
8	6.46×10^{-8}	1.336×10^{-1}	2020	.552	1.13×10^3	6.79×10^3
9	6.63×10^{-8}	1.33×10^{-1}	1230	.62	1.13×10^3	3.64×10^3

1000 100 10 1





within the limits of experimental error. Furthermore, it reveals a small but substantial oscillation in these values.

Heat transfer from droplets to a continuous phase with the liquid system has been studied by Calderbank²² and Goversloot. The relationship obtained by them is presented in fig. 8 along with those of Collier²³ et al. Calderbank²² et al. had a situation similar to present investigation in the sense that they employed falling sessile droplets in acetone-silvered mixture and studied the average convective heat transfer. In the similar manner the experimental data of the present investigation have also been plotted in fig. 8.

However, as figure 8 shows, the data from this investigation are approximately an order of magnitude higher than those of Calderbank et al.²². The results of Collier²³ et al. deviate from the other and appears to merge with the present data when the former is extrapolated to higher Re values.

A comparison with heat transfer from solid sphere reveals that at low Reynolds no, oscillation inside the droplet does not have any appreciable effect on convective phase mass-transfer coefficient. According to Calderbank et al., their data deviated from the solid sphere behaviour above $Re \approx 800$ presumably due to droplet oscillation. If this interpretation is correct then it is to be noted that the droplet oscillation or air shear causes depending upon the system will result in the departure from solid sphere behaviour and may have entirely different effect on the mass-transfer coefficient. The higher positive departure of Collier's results cannot be otherwise explained. Following the same argument it may be said that perhaps the droplet oscillation began at much lower Re in the present

investigation because of large lowering of surface tension as a result of high mass transfer rates. Also a high mass transfer rate may by itself change the correlations.

7. Discussion

It is strongly felt that the present method for the study of mass transfer could give a more exact evaluation of mass transfer rates than the use of a large amount of material. Droplets passed through the thin layer of film. In order to study the possibilities of mass transfer from the droplets to the aqueous phase, an area selected and the model was studied under some representative conditions. All the experiments were conducted at $25 \pm 0.5^\circ\text{C}$ by passing, relatively small droplets of different sizes through aqueous media having various concentrations of glycerol and ferric ion. Initial concentrations in aqueous phase were determined by photographic technique, even by suitable spectroscopy the depletion of ferric ion in the aqueous media were obtained. By suitable relationship mass transfer coefficients were calculated. Diffusion coefficient of ferric ion in the different aqueous media were required. Terminal velocity and residence time for the droplets in the aqueous phase were determined by photographic technique.

The conclusions of the present investigations are summarized as follows:

1) Appreciable amount of mass transfer could not be measured even by photographic when the experiments were conducted at $25 \pm 0.5^\circ\text{C}$ in the present apparatus. By increasing the column height, the residence time for the droplets in the aqueous phase could be increased and appreciable amount of mass transfer could be measured at $25 \pm 0.5^\circ\text{C}$. With a short column, experiments at higher temperature solved the problem.

3) Acoustic studies revealed that a small scattered oscillation exists in all experiments.

4) Spectroscopy data 70 to 80 μ sec. exposed in a double phase revealed that the value of mass-transfer coefficient decreases progressively, the decrease in the concentration of ferric ion. This could be attributed to lowering of diffusion coefficient due to increase of ferric ion concentration.

5) In the case of small droplets, the mass-transfer coefficient decreased with increase in the viscosity of the aqueous phase whereas with oil or droplets, the difference in the mass-transfer coefficient values were slight change of solvent droplet coagulation during the 4 phase, 1-4 solvent phase.

6) Smaller droplets showed more or less as solid sphere while at 100, through the viscosity media, decrease in low viscosity media, oscillation to some extent could be observed. In the case of bigger droplets, severe oscillation in the different viscous media had been observed.

7) Terminal velocity and resistance data for all the droplets in the different aqueous media had been determined and systematic variations had been observed.

8) Photographic studies revealed that the smaller droplets were spherical, their terminal velocity within 1 cm from the top of liquid surface where as 3-3.5 cm in the case of bigger ones.

9) The mass-transfer coefficients were not either magnitude higher than that expected from solid sphere behaviour, probably because of droplet oscillations and possibly due to Marangoni effect.

Abbreviations

α	= area in cm^2
α^*	= area of a sphere whose volume is equal to the volume of ellipsoid in cm^2
β	= concentration in gm/cm^3
β^*	= concentration in $\text{wt.}/\text{vol.}$
D	= diffusivity in $\text{cm}^2/\text{sec.}$
d_1	= diameter of the drop in cm
d_e	= equivalent diameter in cm
d_h	= diameter in horizontal direction in cm
d_v	= diameter in vertical direction in cm
e	= eccentricity of drop $\frac{d_h}{d_v}$
e^*	= eccentricity of drop $\frac{d_{h_1}}{d_{h_2}}$
g	= gravitational acceleration cm/sec^2
k_d	= overall mass-transfer coefficient $\text{cm}/\text{sec.}$
k_{d_1}	= drop phase mass-transfer coefficient $\text{cm}/\text{sec.}$
k_{d_2}	= continuous phase mass-transfer coefficient
v	= terminal velocity $\text{cm}/\text{sec.}$
v_L	= terminal velocity for liquid drop
v_S	= terminal velocity for solid sphere from Stokes law.
r	= radius of the droplet in cm
Re_{de}	= Reynolds number $\frac{\rho v d_e}{\mu}$
Re_{dc}	= Schmidt number $\frac{\mu}{\rho D}$

τ_{th} = theoretical value of $\frac{1}{\omega}$

μ = viscosity

SCALAR VALUES

γ = 4.1868

ρ_0 = density of continuous phase

ρ_D = density for drop phase g/cc

σ = surface tension dyn/cm

ω = frequency of oscillation per sec.

μ_c, μ_D = continuous and drop phase viscosity in poise.

δ = diffusion boundary layer thickness in cm.

References

1. R.O. Kirkner, "Long wavelength, collective liquid interaction", in "Advances in Chemical Physics", Vol. 4, edited by J. J. O'Keefe, Academic Press.
2. V. Debye, Z. Physik, 1924, 24, 188.
3. A. Debye, Z. Physik, 1924, 24, 188.
4. A. Debye and E. Hückel, Z. Physik, 1928, 24, 188.
5. S. Debye, "Advances in Chemical Physics", vol. 4, p. 188.
6. J. Debye et al. Z. Physik, 1928, 24, 188.
7. V. Debye, "Advances in Chemical Physics", vol. 4, p. 188.
8. Debye and Hückel, Z. Physik, 1928, 24, 188.
9. S. Debye et al. Z. Physik, 1928, 24, 188.
10. J. Debye and E. Hückel, Z. Physik, 1928, 24, 188.
11. A. Debye, Z. Physik, 1928, 24, 188.
12. S. Debye et al. Z. Physik, 1928, 24, 188.
13. S. Debye, Canadian Journal of Chemistry, 1928, 24, 188.
14. S. Debye and J. O'Keefe, Z. Physik, 1928, 24, 188.
15. A. Debye and E. Hückel, Z. Physik, 1928, 24, 188.
16. Debye and Hückel, Z. Physik, 1928, 24, 188.
17. Debye and Hückel, Z. Physik, 1928, 24, 188.
18. Debye and Hückel, Z. Physik, 1928, 24, 188.
19. S. Debye, A. Debye and E. Hückel, "International Conference on the Physics and Chemistry of Iron and Steel", Conference proceedings held in 1978, University of T. J. J.

20. G. Inli, in *Advances in Math.*, 1972, 24:141.
21. J. J. O'Connor, in *Advances in Math.*, vol. 22, 1976, p. 1.
22. J. J. O'Connor, in *Advances in Math.*, vol. 22, 1976, p. 141.
23. J. J. O'Connor, in *Advances in Math.*, vol. 22, 1976, p. 141.
24. J. J. O'Connor, in *Advances in Math.*, vol. 22, 1976, p. 141.
25. J. J. O'Connor, in *Advances in Math.*, vol. 22, 1976, p. 141.
26. J. J. O'Connor, in *Advances in Math.*, vol. 22, 1976, p. 141.
27. J. J. O'Connor, in *Advances in Math.*, vol. 22, 1976, p. 141.
28. J. J. O'Connor, in *Advances in Math.*, vol. 22, 1976, p. 141.
29. J. J. O'Connor, in *Advances in Math.*, vol. 22, 1976, p. 141.
30. J. J. O'Connor, in *Advances in Math.*, vol. 22, 1976, p. 141.

100

There is no one in the room who is not a member of the same family.

This image shows a single sheet of white paper with horizontal blue or grey ruling lines. A vertical margin line is present on the left side, creating a narrow left margin. The paper appears to be from a notebook or a standard ruled document. There are some faint smudges and shadows across the surface, particularly near the top and bottom edges.

ME-1971-M-CHA-MPS